AD-A159 109   EXPERIMENTAL INVESTIGATION OF MAGNESIUM COMBUSTION IN   1/1
STEAM(U) NAVAL POSTGRADUATE SCHOOL MONTEREY CA
Y CHOZEV ET AL. JUL 85 NPS67-85-004CR
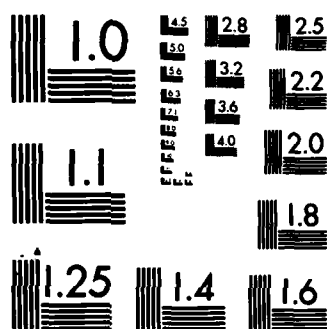
UNCLASSIFIED   F/G 21/2   NL

END
FILMED
DTIC

MICROCOPY RESOLUTION TEST CHART

NATIONAL BUREAU-OF STANDARDS-1963-A

NPS67-85-004CR

NAVAL POSTGRADUATE SCHOOL
Monterey, California

CONTRACTOR REPORT

EXPERIMENTAL INVESTIGATION OF MAGNESIUM

COMBUSTION IN STEAM

Yair Chozev and Jacob Kol

July 1985

Approved for public release; distribution unlimited.

Prepared for: Naval Surface Weapons Center
White Oak Laboratories
Silver Springs, MD 20910

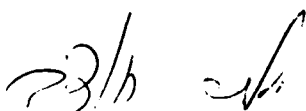5 09 12 037

NAVAL POSTGRADUATE SCHOOL
Monterey, California

RADM R. H. Shumaker   D. A. Schrady
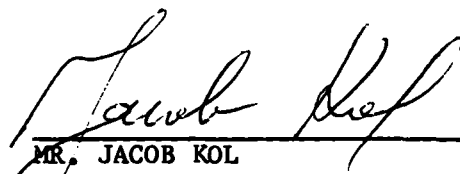Superintendent   Provost

The work reported herein was carried out for the Naval Postgraduate School
by Mr. Jacob Kol under Contract N62271-84-M-3357 and Mr. Yair Chozev under
Contract N62271-84-M-3055. The work presented in this report is in support of
"Underwater Shaped Charges" sponsored by the Naval Surface Weapons Center. The
work provides experimental investigation of magnesium combustion in steam. The
project at the Naval Postgraduate School is under the cognizance of
Distinguished Professor A. E. Fuhs who is principal investigator.

Reproduction of all or part of this report is authorized.
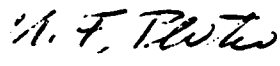
Prepared by:

_____   _____
MR. YAIR CHOZEV   MR. JACOB KOL
Research Contractor   Research Contractor

Reviewed by:

_____   _____
ALLEN E. FUHS   M. F. PLATZER
Distinguished Professor   Chairman, Department of Aeronautics

Released by:

_____
J. N. DYER
Dean of Science and Engineering

REPORT DOCUMENTATION PAGE		READ INSTRUCTIONS BEFORE COMPLETING FORM
1. REPORT NUMBER NPS67-85-004CR	2. GOVT ACCESSION NO. *A159109*	3. RECIPIENT'S CATALOG NUMBER
4. TITLE *(and Subtitle)* Experimental Investigation of Magnesium Combustion in Steam		5. TYPE OF REPORT & PERIOD COVERED Contractor's Report Dec. 1984 – May 1985
		6. PERFORMING ORG. REPORT NUMBER
7. AUTHOR(s) Yair Chozev and Jacob Kol		8. CONTRACT OR GRANT NUMBER(s) N62271-84-M-3055 N62271-84-M-3357
9. PERFORMING ORGANIZATION NAME AND ADDRESS Naval Postgraduate School Monterey, CA 93943-5100		10. PROGRAM ELEMENT, PROJECT, TASK AREA & WORK UNIT NUMBERS
11. CONTROLLING OFFICE NAME AND ADDRESS		12. REPORT DATE July 1985
		13. NUMBER OF PAGES 44
14. MONITORING AGENCY NAME & ADDRESS(*if different from Controlling Office*) Naval Postgraduate School Monterey, CA 93943-5100		15. SECURITY CLASS. *(of this report)* UNCLASSIFIED
		15a. DECLASSIFICATION/DOWNGRADING SCHEDULE

16. DISTRIBUTION STATEMENT *(of this Report)*

Approved for public release; distribution unlimited.

17. DISTRIBUTION STATEMENT *(of the abstract entered in Block 20, if different from Report)*

Accession For

NTIS GRA&I ☒
DTIC TAB ☐
Unannounced ☐
Justification

By
Distribution/
Availability Codes

Dist	Avail and/or Special
A-1	

DTIC COPY INSPECTED 3

18. SUPPLEMENTARY NOTES

19. KEY WORDS *(Continue on reverse side if necessary and identify by block number)*

Combustion of Magnesium, Burning of Magnesium, Combustion in Steam, Burning in Steam, Combustion Temperature, Magnesium, Magnesia.

20. ABSTRACT *(Continue on reverse side if necessary and identify by block number)*

This paper presents a summary of the experimental results and studies of magnesium combustion in steam. The major subject of these studies was to measure the temperature of magnesium particles after the particles had been ejected from an exploding wire. The distribution of particle temperature along the track was measured by the two-color photo-pyrometry method (TC-PPM). In this method, absolute emissivity and velocity of the particles are not

DD FORM 1473 EDITION OF 1 NOV 65 IS OBSOLETE
1 JAN 73
S/N 0102-LF-014-6601

needed due to differential measurements of radiation energy by density of film exposed to the event. All the other existing methods for moving burning particles require the knowledge of emissivity and velocity correction data. A scanning microdensitometer served as a major data reduction tool in analyzing the film density due to the particle tracks as recorded on calibrated film. The TC-PPM was calibrated using a standard lamp prior to particle temperature measurements.

The initial temperature of the particle ejection from the plasma and at the beginning of combustion is 3430 K ± 9.1%. At the initial phase of combustion, the particle consists of pure magnesium with spectral emissivity of about 0.25. During the combustion process, magnesium oxide is formed locally on the particle surface. The oxide is in liquid state with emissivity of 0.9. In the second stage of combustion there are changes on the particle surface in correlation with optical density variation and explained by emissivity variations due to peeling of the oxide film and exposure of the pure magnesium surface. Solidification of the particle, which is magnesium oxide, is observed at the measured temperature of 3125 K ± 5.7%. This temperature is near the melting point of magnesia. At the solidification point, abrupt reduction of radiation occurs due to the change of magnesia emissivity from 0.9 (at liquid state) to 0.3 (at solid state).

The spearpoint effect, which is known in the literature as the Blick Effect, was observed at the end of the particle track. The particle supercools below the normal freezing point and then suddenly crystallizes. The measured temperature at the crystallization point is 2840 K ± 5.7%.

TABLE OF CONTENTS

LIST OF FIGURES

LIST OF TABLES

ABSTRACT

This paper presents a summary of the experimental results and studies of magnesium combustion in steam. The major subject of these studies was to measure the temperature of magnesium particles after the particles had been ejected from an exploding wire. The distribution of particle temperature along the track was measured by the two-color photo-pyrometry method (TC-PPM). In this method, absolute emissivity and velocity of the particles are not needed due to differential measurements of radiation energy by density of film exposed to the event. All the other existing methods for moving burning particles require the knowledge of emissivity and velocity correction data. A scanning microdensitometer served as a major data reduction tool in analyzing the film density due to the particle tracks as recorded on calibrated film. The TC-PPM was calibrated using a standard lamp prior to particle temperature measurements.

The initial temperature of the particle ejection from the plasma and at the beginning of combustion is 3430 K ± 9.1%. At the initial phase of combustion, the particle consists of pure magnesium with spectral emissivity of about 0.25. During the combustion process, magnesium oxide is formed locally on the particle surface. The oxide is in liquid state with emissivity of 0.9. In the second stage of combustion there are changes on the particle surface in correlation with optical density variation and explained by emissivity variations due to peeling of the oxide film and exposure of the pure magnesium surface. Solidification of the particle, which is magnesium oxide, is observed at the measured temperature of 3125 K ± 5.7%. This temperature is near the melting point of magnesia. At the solidification point, abrupt reduction of radiation occurs due to the change of magnesia emissivity from 0.9 (at liquid state) to 0.3 (at solid state).

vi

Cont'd

The spearpoint effect, which is known in the literature as the Blick Effect, was observed at the end of the particle track. The particle supercools below the normal freezing point and then suddenly crystallizes. The measured temperature at the crystallization point is 2840 K ± 5.7%.

ACKNOWLEDGEMENT

The authors acknowledge the valuable help, cooperation and guidance of
Professor Allen E. Fuhs during this work.

viii

I. INTRODUCTION

The energy released by metals burning in steam has several important applications including torpedo propulsion, nuclear reactor safety, underwater vehicles, underwater ordnance, etc. This report continues the studies that were performed by Hallenbeck [1], Berger et. al., [2] and Kol et. al., [3] at the Naval Postgraduate School which are related to the investigation of underwater shaped charges. Only a few articles dealing with combustion of magnesium in steam have been published; however, none of them were dealing with temperature of magnesium particles burning in steam. The model for magnesium burning in $Ar-O_2$ mixture that was proposed by Bruzustowski and Glassman [4] and [5] assumed the following characteristics for magnesium combustion:

(a) At the highest range of burning rates, the flame temperature will be fixed at the boiling point of the oxide, and the state of the oxide produced will be variable with some oxide always in the condensed state.

(b) The diffusion of oxygen toward the flame zone is affected by the condensed products of combustion which cannot diffuse and must be convected with the bulk gas motion.

(c) The existence of condensed species in the flame zone at the high temperature level makes thermal radiation important both in the rate of heat feedback from the flame to the evaporating surface and in the rate of heat loss from the flame to the surroundings.

(d) The evaporation of metal from the surface may not be very fast in comparison with the diffusion processes occurring in the gas phase.

The degree of dissociation of the products in the flame zone depends upon the balance between heat released by chemical reaction and heat loss by radiation and conduction. For both metal and hydrocarbons the inward

1

diffusion of oxygen is hindered by the outward diffusion of gaseous products. Grosse and Conway [6] found that the upper limit of the burning temperature of magnesium in oxygen was 3350 K. This result matches the assumption "a" that was made in [4] and [5].

Florko et. al., [7] measured the spectrum of magnesium particle burning in air and the temperature distribution along the distance from the particle center. The temperatures were obtained by using different techniques as follows:

(a) The surface temperature of the particle was 1400 K measured by using direct thermocouple method.

(b) The maximum intensity of continuous spectrum temperature was 2600 ± 200 K at distance of $2r_0$ (r_0 is the particle radius).

(c) The maximum burning temperature of 2950 ± 200 K was obtained at the distance of $3r_0$ using the relative distribution of the population of the vibrational levels of the excited electronic state assuming Boltzmann distribution.

All of the above experiments were conducted in different conditions compared to experiments reported herein. Therefore one may expect differences in the experimental results. In this report are summarized experimental studies of magnesium burning in steam which included burning temperature and burning behavior.

2

II. FILM DENSITY VERSUS TEMPERATURE - THEORETICAL MODEL

The exposure of the film, H , ergs/cm^2 , due to radiation from a burning particle was derived in Berger et. al., [2] as follows:

$$H = \frac{T_f \Delta\lambda \varepsilon W_{bb} \pi D}{4f^2 V(t)}$$ (1)

where

T_f — Transmissivity of the filters = 0.57 @ 649 nm and 0.58 @ 482 nm

$\Delta\lambda$ — Bandwidth of the filters = 11.4 nm @ 649 nm and 7.1 nm @ 482 nm

ε — Emissivity of the particle (see equation (2))

W_{bb} — Black body radiant exitance $[\frac{erg}{cm^2 s\ \mu m}]$

D — Diameter of the particle = 385 μm

f — f-number of the camera (see Table 1)

$V(t)$ — Velocity of the particle* [m/s]

* For the above model initial velocity of 24 m/s was used.

During the combustion process, a liquid oxide film is gradually formed around the pure magnesium; accordingly there is a continuous variation of particle emissivity from pure liquid magnesium emissivity (ε_m) to liquid oxide emissivity (ε_{OX}) . An emissivity variation is approximated by linear interpolation as follows:

$$\varepsilon_p(T) = \varepsilon_m[1 + \frac{\varepsilon_{OX} - \varepsilon_m}{\varepsilon_m} (\frac{T_0 - T}{T_0 - T_B})]$$ (2)

where

ε_{OX} — Magnesium emissivity (liquid) = 0.25 @ $T < T_B$ and 0.9 @ $T > T_B$

ε_m — Magnesium emissivity (liquid) = 0.25

ε_p — Interpolated particle emissivity

T — Particle temperature during combustion

T_0 — Initial particle temperature (3350 K)

T_B — Temperature at burnout (3075 K)

3

According to Buber et. al., [8], the emissivity of liquid magnesia above temperature of 3075 K is 0.9. According to Touloukian and DeWitt [9], the emissivity of liquid magnesium is 0.2.

Film optical density at $\lambda_1 = 649$ nm can be calculated by the following expression:

$$D_1 = K_1 \log_{10} H_1 - K_1 \log_{10} H_{min} + D_0 \qquad (3)$$

where
K_1 — Slope of $\log_{10} H$ curve at 649 nm

H_{min} — Minimum exposure energy at gross fog

D_0 — Density for gross fog of the film

H_1 — Film exposure energy from Equation (1) at 649 nm

Accordingly, film optical density at $\lambda_2 = 482$ nm is given by:

$$D_2 = K_2 \log_{10} H_2 - K_2 \log_{10} H_{min} + D_0 \qquad (4)$$

where
K_2 — Slope of $\log_{10} H$ curve at 482 nm

H_2 — Film exposure energy from Equation (1) at 482 nm

Using Equations (1) to (4), data for Kodak recording film 2475 [10], and optical instrumentation (see Section III), Figure 1 was obtained. Curves from 1 to 6 of Figure 1 describe film optical density versus temperature for constant emissivity value. Curves from 7 to 12 describe film optical density versus temperature assuming a linear increase of a particle emissivity given by Equation (2). An important observation is that the maximum measured density will be expected near 3200 K. The density will remain high until a temperature of 3075 K (melting temperature of magnesia). Then the density will decay due to the solidification of magnesia.

4
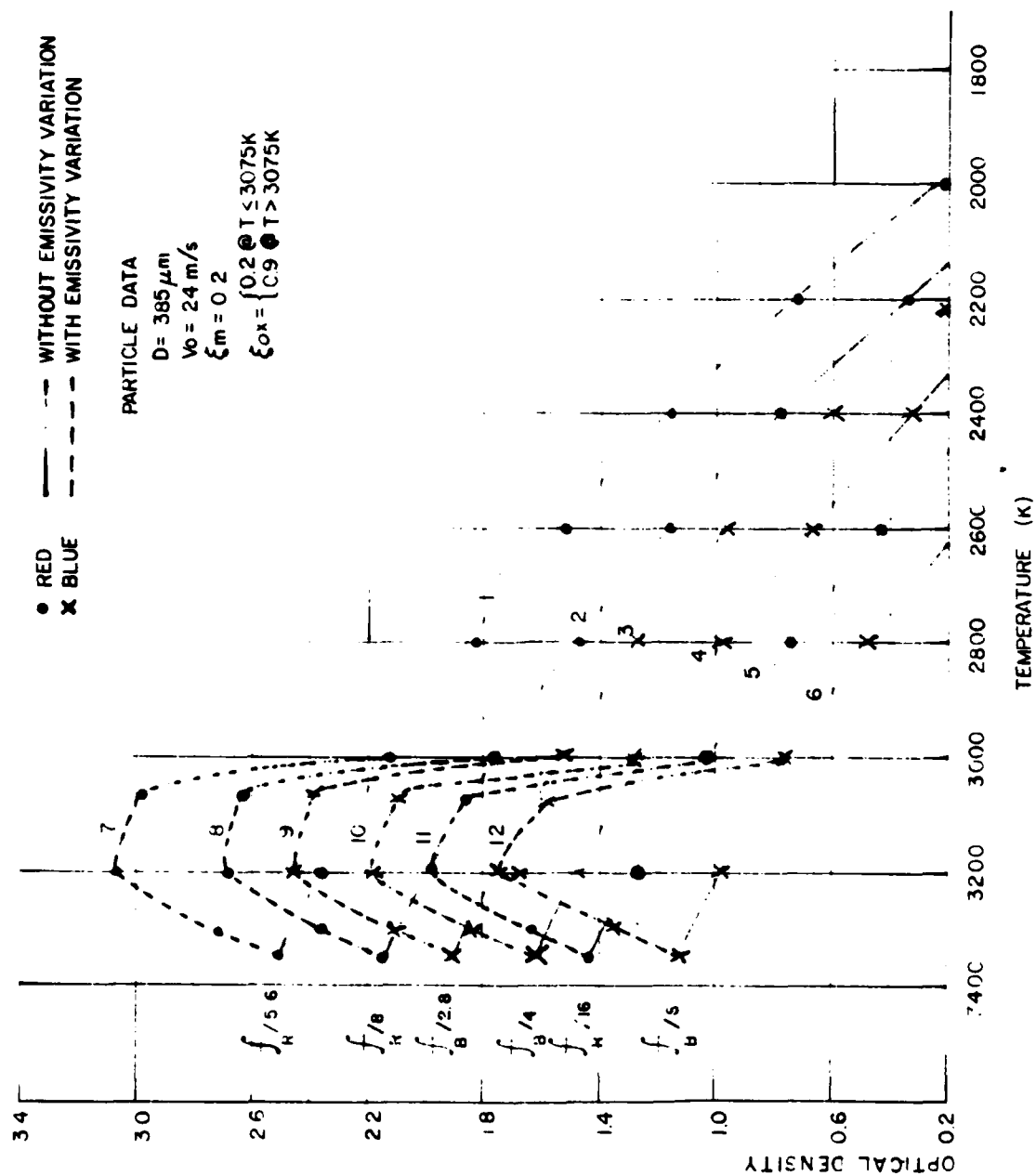
Figure 1. Theoretical Optical Density of the Particle Image Versus Temperature

5

III. EXPERIMENTAL

The experiments were conducted in pressure vessel which consisted of a twelve inch high stainless steel cylinder, 10.75 inches diameter with four evenly spaced, 5 inch diameter observation ports welded into its circumference. One inch thick, Schlieren quality, Borosicalate crown glass (BK-7) was installed in each port. Two Watlow Band Heaters were used to heat the apparatus to operating temperature and four additional Watlow Heaters were mounted on observation ports in order to prevent steam condensation during experiments. An Omega model 157 Digital Controller was used for temperature stabilization. The experiments were conducted in pressure range of 19 to 32 psi and steam temperature of 180°C. Thermocouples were mounted in different locations inside the chamber to measure the internal temperature.

The magnesium particles were generated by the exploding wire technique. The 5 cm length wire was mounted between two holders and the ignition energy transfered to the wire was about 90 Joule. The direct energy measurements included the calibrated shunt current measurement and direct voltage measurements across the wire.

Particle temperature was measured by two-color photo-pyrometry method (TC-PPM, see Berger et. al., [2]). An Optronics Microdensitometer Photoscan system P-1000 was used for optical density measurements. Two still Pentax 35 mm cameras were used for two-color (482 nm, 649 nm) photography of the events. Kodak 2475 recording film was calibrated for a detailed graph of film density versus exposure. 1.5 millimeter diameter magnesium wire with purity of 99.998% was used in the experiments. Using the TC-PPM method one can solve Equation (5) using measured densities for $\lambda_1 = 649$ nm and $\lambda_2 = 482$ nm.

6

$$T = \frac{C_2\left(\frac{1}{\lambda_2} - \frac{1}{\lambda_1}\right)}{\left(\frac{D_1 - D_o}{K_1} - \frac{D_2 - D_o}{K_2}\right)\ln 10 - \ln A} \qquad (5)$$

where

$$A = \frac{T_{f1}\ \lambda_2^5\ \Delta\lambda_1\ f_2^2\ \varepsilon_1}{T_{f2}\ \lambda_1^5\ \Delta\lambda_2\ f_1^2\ \varepsilon_2} \simeq \frac{T_{f1}\ \lambda_2^5\ \Delta\lambda_1\ f_2^2}{T_{f2}\ \lambda_1^5\ \Delta\lambda_2\ f_1^2}$$

Assuming that $\frac{\varepsilon_1(649)}{\varepsilon_2(482)} = 1$. The assumption that $\varepsilon_1/\varepsilon_2 \simeq 1.0$ is important.

See error calculations in [2]. For magnesium particles temperature measurement the following parameters were used:

$\lambda_1 = 649$ nm ; $\lambda_2 = 482$ nm;

$\Delta\lambda_1 = 11.4$ nm ; $\Delta\lambda_2 = 7.1$ nm;

$T_{f1} = 0.57$; $T_{f2} = 0.58$

$K_1 = 1.2$; $K_2 = 0.85$

$f_1 = 5.6$; $f_2 = 2.8$

$C_2 = 14388$ μm K

Using the above parameters, Equation (5) will be as follows:

$$T = \frac{3338}{\frac{D_1 - D_{01}}{K_1} - \frac{D_2 - D_{02}}{K_2} + 1.056} \qquad (6)$$

7

The camera setting and testing conditions for the studies of magnesium
particles burning in steam are shown in Table 1.

Table 1. Camera Setting and Testing Conditions for Magnesium Burning in Steam

TEST NO.	AMBIENT TEMP. (°F)	PRESSURE (PSI)	CAMERA 1				CAMERA 2			
			LENS (mm)	f NUMBER	λ (nm)	DISTANCE (cm)*	LENS (mm)	f NUMBER	λ (nm)	DISTANCE (cm)*
10	363	21	85	16	649	85	55	8	482	65
11	360	22	85	8	649	85	55	4	482	65
12	373	22.5	85	8	649	85	55	4	482	65
13	382	22	85	8	649	85	55	4	482	65
14	367	30	85	8	649	85	55	4	482	65
15	383	29	85	5.6	649	85	55	2.8	482	65
16	374	23	85	5.6	649	85	55	2.8	482	65
17	390	23	85	5.6	649	85	55	2.8	482	65
18	347	28	85	5.6	649	85	55	2.8	482	65
19	377	32	85	5.6	649	85	55	2.8	482	65
1	360	20	85	8	649	85	55	4	450	65
2	360	20	85	8	649	85	55	4	450	65
3	365	20.5	85	8	649	85	55	4	450	65
4	340	21	85	8	649	85	55	4	450	65
5	355	20	85	8	649	85	55	4	450	65
6	325	21.5	85	8	649	85	55	4	450	65
7	355	20	85	5.6	649	85	55	2.8	450	65
8	360	20	85	5.6	649	85	55	2.8	450	65
9	345	20	85	5.6	649	85	55	2.8	450	65
10	370	20.5	85	5.6	649	85	55	2.8	450	65
11	360	20	85	5.6	649	85		2.8	450	65
12	365	21	85	5.6	649	85	55	2.8	450	65
1	360	19	85	8	649	85	55	8	599	55
2	375	23	85	8	649	85	55	8	599	55
3	365	23	85	8	649	85	55	8	599	55
4	350	23	85	8	649	85	55	8	599	55
5	395	21.5	85	8	649	85	55	8	599	55
6	350	20.5	85	8	649	85	55	11	599	55
7	390	21.5	85	8	649	85	55	5.6	599	55
8	380	20	85	8	649	85	55	8	599	55
9	385	23	85	8	649	85	55	11	599	55
10	370	25	85	8	649	85	55	8	599	55
11	375	22	85	8	649	85		8	599	55
12	365	23	85	8	649	85		8		
13	365	23	85	8	649	85	55	8	599	55
14	380	21	85	8	649	85	55	11	599	55
15	370	22	85	8	649	85	55	8	599	55
16	370	20	85	8	649	85	55		599	55
17	390	25	85	11	649	85		11	599	55
18	370	20.5	85	11	649	85	55	8	599	55
19	365	20	85	11	649	85				

* Distance is the distance of camera 1 and 2 from the source of particles (wire).

9

IV. RESULTS AND DISCUSSION

A. Photographs of Magnesium Particles Burning in Steam

As discussed previously, the two-color photo-pyrometry method (TC-PPM) requires recording the particle image by calibrated film. Figures 2 and 3 are photographs produced from one exposure in the blue and one in the red wavelength regions.

Figure 2 is the event as photographed with blue filter at 482 nm using an open shutter. Note the ball of plasma formed by the rupture of the magnesium wire. Also note the particle tracks emitting from the plasma. In the original photographs, the spearpoint or Blick Effect can be seen.

Figure 3 is the corresponding photograph for the same event observed with the red filter at 649 nm. The image of Figure 3 is the mirror image of Figure 2. The two cameras observe the exploding wire through observation ports which are 180° apart, i.e., the cameras record the event from opposite directions.

B. Temperature Measurement for Particle Combustion in Steam

Particle temperature measurements were performed by TC-PPM method which was calibrated prior to the particle combustion experiments by using calibrated quartz-halogen-tungsten lamp with total measured errors of ± 5.7 percent.

The two film density distributions (in 649 nm and 482 nm wavelengths) along the particle track as function of normalized distance from plasma (distance in experiment = normalized distance x 0.1315 mm) are shown in Figure 4.

The temperature variation along the burning particle track can be seen in Figure 5 and summarized as follows:

The burning particle is ejected from very high temperature plasma. At the

10

Figure 2. Exploding magnesium wire photographed with blue filter at 482 nm.

Figure 3. Exploding magnesium wire photographed with red filter at 649 nm.

end of the particle track, an abrupt change in measured temperature occurs

from 3125 K ± 5.7% to 1991 K ± 5.7% as is shown in Figure 5.

At normalized distance less than 120, the temperature calculation was not

possible due to high intensity radiation at λ_2 = 482 nm. Further discussion

concerning this phenomenon will be given at next paragraph.

C. Burning Behavior of Magnesium Particles in Steam

Five different tracks of film density variation are shown in Figure 4 and

in the Appendix from Figures 11a to 11d. According to the film density

variation of a representative track in Figure 4, one can distinguish three

different burning regions as follows:

The first region, for normalized distance less than about 120 is

characterized by D_2 (blue) greater or equal to D_1 (red). The second

region, for normalized distance from 120 to 210 (approximately) is

characterized by continuously growing difference between the red and the

blue densities $(D_1 - D_2)$. In the third region, for normalized distance

greater than 210, the difference between densities is decreasing.

a. First Region - Blue Radiation Interference

In order to explain the source of the blue radiation interference in

the first region, the following studies were performed:

1. By examination of the microdensitometer results for this region,

higher blue densities were observed at longer radial distances

from the plasma center than at red densities. It is shown in

Figure 6.

2. Magnesium wires burning in steam were photographed by 35 mm color

film, and a blue glowing "cloud" was observed around the plasma

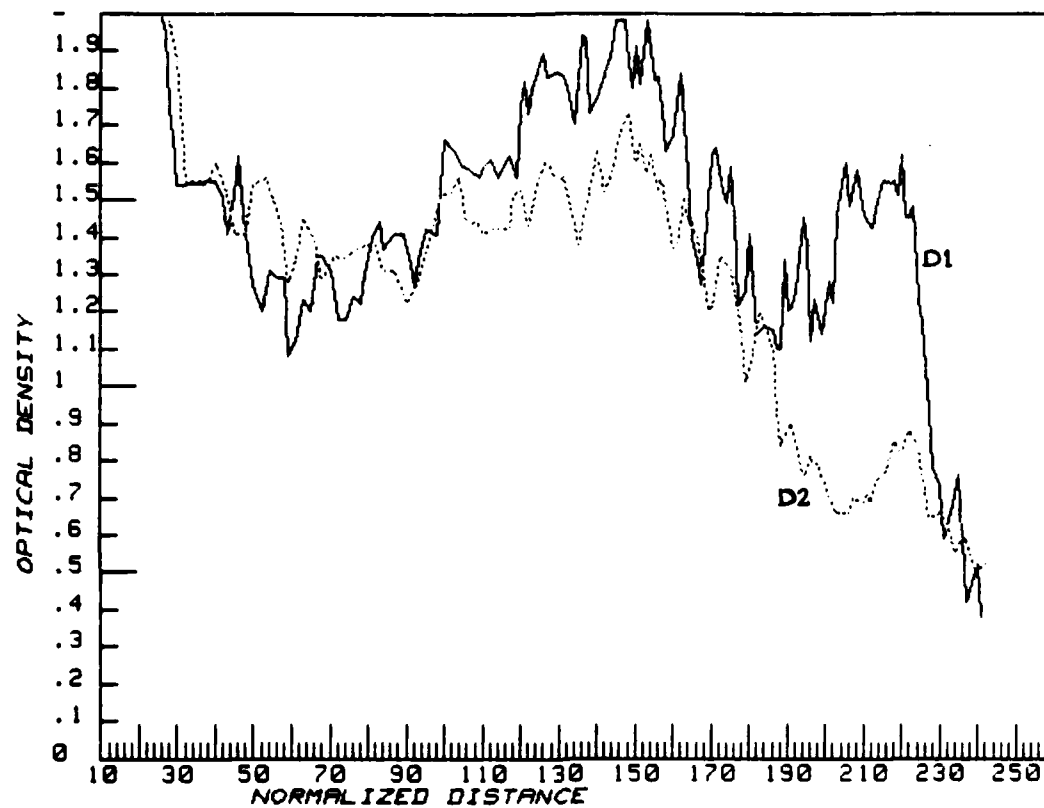with streaks propagating outwards.

12

Figure 4. Measured film density as a function of normalized distance along a typical particle track.
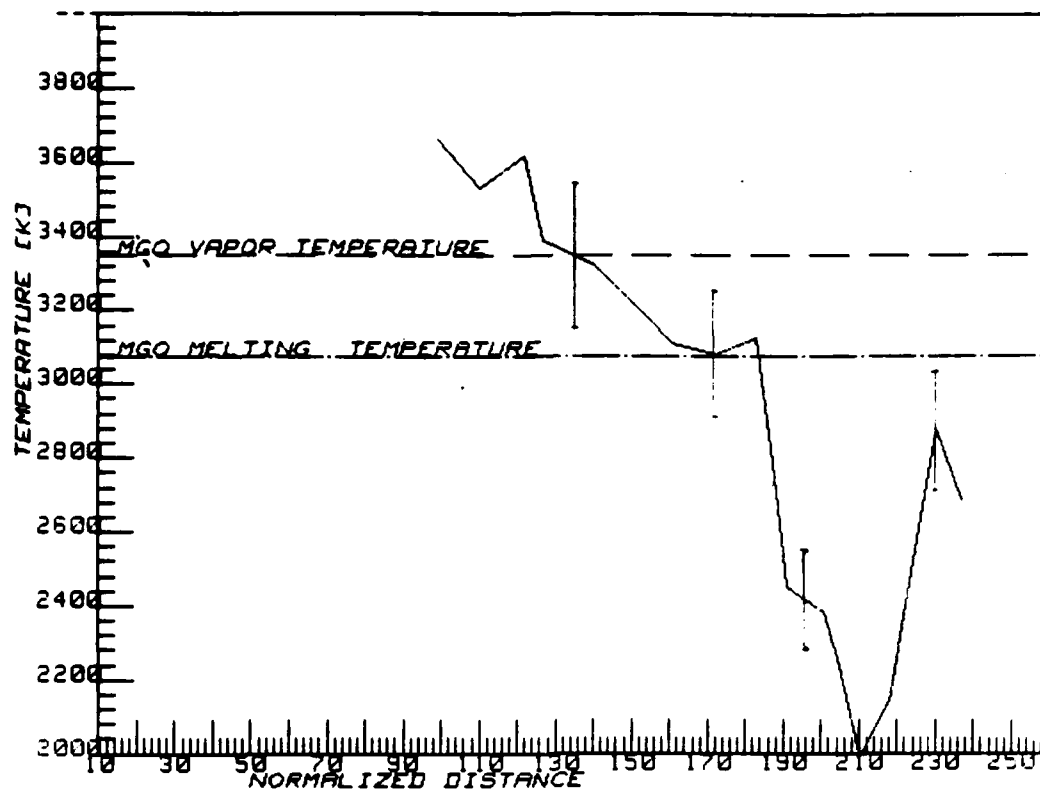
13

Figure 5. Typical temperature variations of magnesium particle in steam along the particle track (based on the densities of Figure 4).
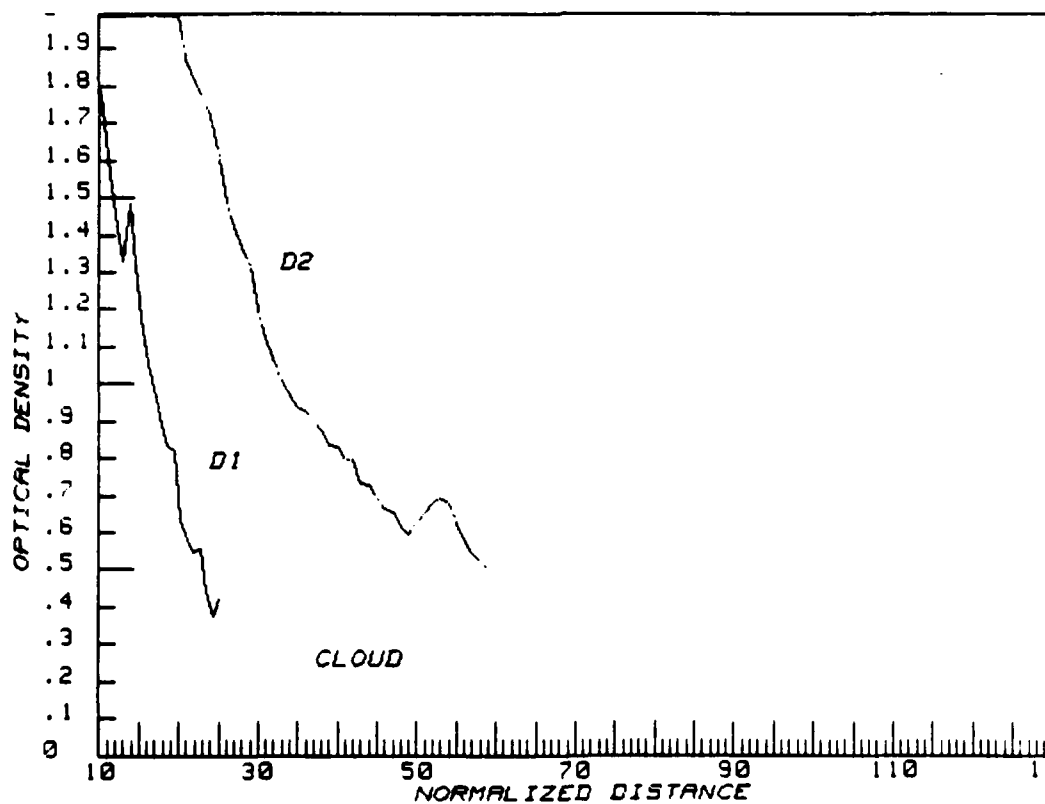

Figure 6. Optical density due to cloud of particles versus distance along particle track.

14

3. The spectroscopic studies that were performed by Brzustowski and
    Glassman [5] showed that when magnesium ribbons are burning in an
    ambient gas consisting of 40% oxygen and 60% argon at a pressure
    of 300 mm Hg, the reaction emits Mg* and MgO* spectral lines. The
    most relevant lines are the excited MgO peak lines from 491 to
    501 nm. Other strong lines were the green lines of Mg* ($\sim$517 nm).

4. The possibility of emission from other various components is
    summarized using [11], [12] and [13] in Table 2. As is shown
    there is no evidence of other spectral lines such as of MgOH and
    O_2.

5. In order to investigate the source of the blue emission around the
    plasma there were performed experiments of igniting magnesium
    wires in two different pressures of air: 0.25 and 14 psi. The
    35 mm color photographs showed that in the higher pressure of air,
    the blue cloud was about the same size as in steam, considering
    the difference of pressures. In the lower pressure atmosphere,
    the blue "cloud" was significantly smaller, but there was an
    interface of green radiation between the white plasma and the blue
    (smaller) "cloud". The behavior of ignited magnesium wires is
    shown in Figure 7. The green radiation indicates magnesium vapor
    (see (3) above) around the plasma in the low pressure air.

15
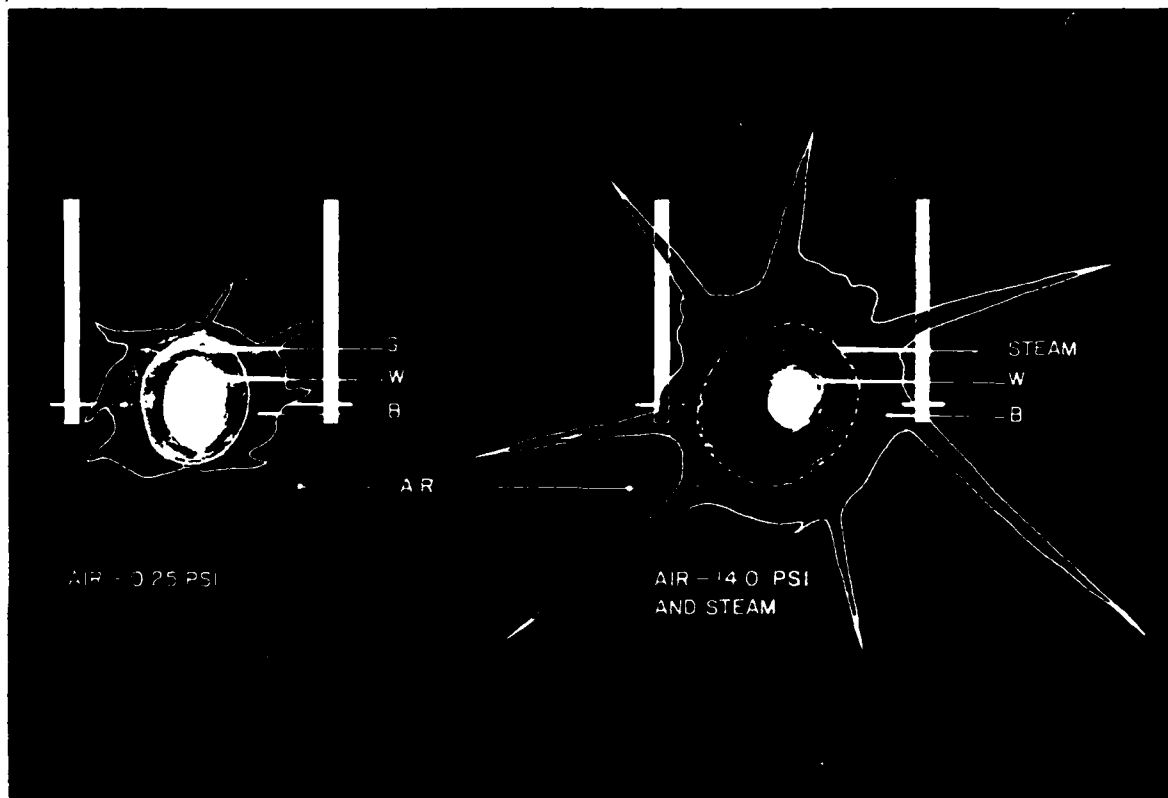
Figure 7. Plasma description in air and in steam.

G - Green

B - Blue

W - White

16

Table 2. Spectral Lines of Mg, O, H, H_2, MgH and MgO from 470 nm to 490 nm.

COMPOUND	λ(nm)	RELATIVE INTENSITY	eV
Mg	470.3	7	7.0
Mg^+	474.0	5	14.2
Mg^+	485.1	7	14.2
O	480.3	4	13.3
	477.4	5	13.3
	477.3	4	13.3
O^+	489.1	4	28.8
	487.2	5	31.4
	485.7	3	28.8
	475.1	4	28.8
	471.0	5	28.8
H	(H_β)486.1	500 (?)	12.7
H_2	487.3	8-10	
	485.7	8-10	
	484.9	8-10	
	482.3	8-10	
	476.4	8-10	
MgH	484.5		
MgO	481.9	3	
	481.0	3	
	480.1	3	

6. By using the logical flow graph in Figure 8 and the condensed data from 1 to 5, one can conclude that the designated path in Figure 8 is the most reasonable for magnesium burning in steam, and the possible sources of blue radiation are MgO^*, O^* and O^+. By comparing the burning of Mg to other metals burning in steam such as $A\ell$, Ta, Zr and pyrofuze no evidence of blue radiation was observed around the plasma; therefore, the choice of O^* and O^+ is not relevant for magnesium. In addition, the excitation energies of O^* and O^+ (13.3 eV, 30 eV respectively) are much higher then excitation energy of MgO (2.5 eV); therefore we believe that excited MgO is the source of the blue radiation as was found by Brzustowsky and Glassman in air [5].

7. The interference of the "cloud" of the blue radiation was measured by microdensitometer up to a normalized distance of 60 (Figure 6), but the interference along the tracks is up to normalized distance of 120. One possible reason for this behavior is as follows: The "cloud" (smoke) of blue radiation consists of small particles distributed along the track ($10 \mu m$ and less [5]), which are cooling faster than the measured big particles ($100 \mu m - 400 \mu m$) [1] therefore one can conlcude that excited MgO exists along particle track up to normalized distance of 120 due possibly to high initial heat transfer from plasma. The particle gradually transfers the heat to the ambient gas and finally, at the end of first region, excited MgO does not exist and MgO occurs in the ground state.

18
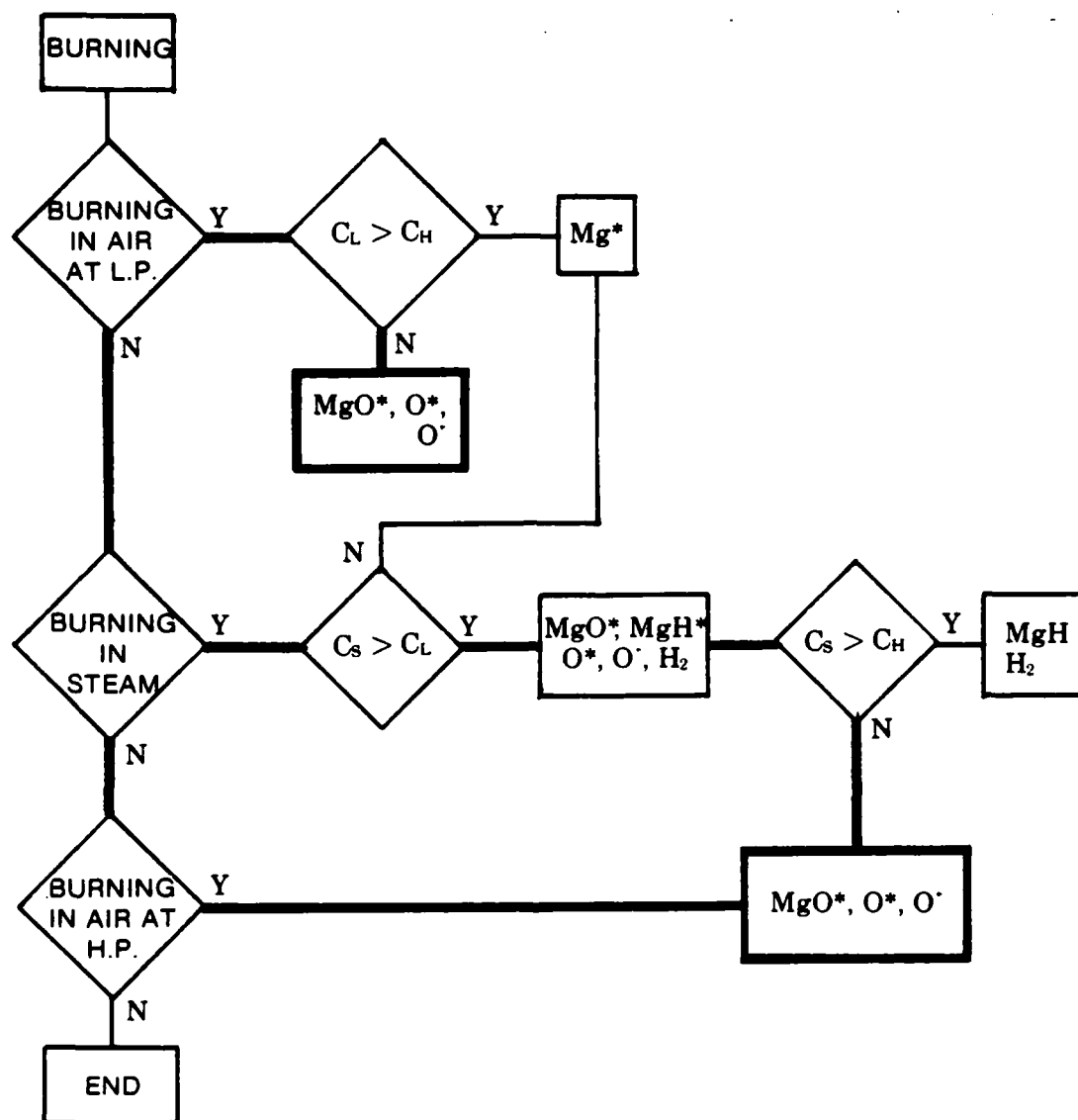
C_L - Diameter of the blue "cloud" in air at low pressure

C_H - Diameter of the blue "cloud" in air at high pressure

C_S - Diameter of the blue "cloud" in steam at high pressure

Figure 8. Logical flow graph for magnesium experiments in steam (20 psi) and air at two different pressures (0.25, 14 psi).

19

b. Second Region - Changes in Magnesium Particle Surface

This region begins at normalized distance of 120 and ends at normalized distance of 210 (see Figure 4). There is observed increase of measured density of the film as was photographed with blue filter at 482 nm and with red filter at 649 nm. The increase of the density from normalized distance of 120 to 150 could be related to an increase of emissivity due to successive covering of the particle by oxide. This behavior also was obtained by the theoretical studies as was described in Figure 1. Photographs 2 and 3 show changes on the particle surface, and there is correlation between these changes and the rapid changes in the measured densities of the film in Figure 4. Derevyaga et. al., [14] suggest the following explanation to those changes: The droplet begins to lose the oxide film; a zone of vapor gas reaction forms about it; and the brightness of the radiation from the particle increases. By correlating this oxide peeling to emissivity variations, while the variation of the temperature is only 305 K, one can calculate the change in emissivity by using equation (6) that was developed in [2]:

$$\frac{\varepsilon_{ox}}{\varepsilon_m} = \log_{10}^{-1} \frac{D_{max}-D_{min}}{K_i} \tag{6}$$

where D_{max} - The maximum density of the film

D_{min} - The minimum density of the film

K_i - The slope of the logH curve

By using the measured results of the film densities, one can obtain the ratio of emissivities $\varepsilon_{ox}/\varepsilon_m$ as follows:

at 482 nm the ratio was from 1.7 to 2

at 649 nm the ratio was from 1.81 to 2.28

20

Assuming that the emissivity at the steady state of magnesia at temperature above 3075 K is 0.9 (Buber et. al., [8]) the average change in emissivity will be from 0.9 to 0.486 at 482 nm and from 0.9 to 0.44 at 649 nm. Those results are comparable to the results that were published by Touloukian and DeWitt [9] for liquid magnesium (ε_m = 0.2 - 0.25) considering the assumption that the oxide peeling is not complete.

c. Third Region - Near The Spearpoint

Along the track, in normalized distance greater than 210, the radiation from the particle becomes less intense, then brightens, gradually loses intensity again and then disappears. An explanation of this phenomena based on super cooling of the molten oxide particle has been discussed by Nelson et. al., [15]. According to this mechanism, when the burning is near completion, the particle temperature is below the normal freezing point, i.e., the particle is in a supercooled condition. Then the particle suddenly crystallizes and increases to a temperature near but below the equilibrium melting temperature with an abrupt increase of thermal emission. Finally, the particle cools gradually to ambient temperature.

The abrupt increase of temperature to 2840 K ± 5.7% was measured by TC-PPM for magnesium burning particle in steam. The amount of temperature increase, ΔT, can be calculated from heat of solidification as follows:

$$\Delta T = \frac{\Delta H_f}{C_p} = 1350 \text{ K}$$

where ΔH_f, heat of solidification, 459 cal/gm, C_p, heat capacity of magnesia at 2500 K, 0.34 cal/gmK.

21

The calculated amount of temperature increase and the measured amount
of temperature increase of 1130 ± 5.7% are comparable.

D. Temperature Investigation by Using Different Filters

In order to eliminate the influence of the radiation in 482 nm, there
were performed a series of experiments in the following wavelengths:

1) 450 nm and 649 nm

2) 599 nm and 649 nm.

By using the first set of filters in the experiments (Table 1) the influence
of spectral line radiation was still significant. By using the second set of
filters in other experiments (Table 1) there were measured optical densities
by using a microdensitometer and are shown in Figure 9. Calculated
temperatures are shown in Figure 10 by using the following measured parameters
of the 599 nm filter:

$T_f = 0.535$

$\lambda = 599$ nm

$\Delta\lambda = 10.5$ nm

Therefore one can conclude that the temperature for magnesium burning in steam
in first region is close to the MgO vapor temperature. The total error for
temperature measurement (see for details [2]) in this set of filters is 9.1%
and is shown in Figure 10.

22

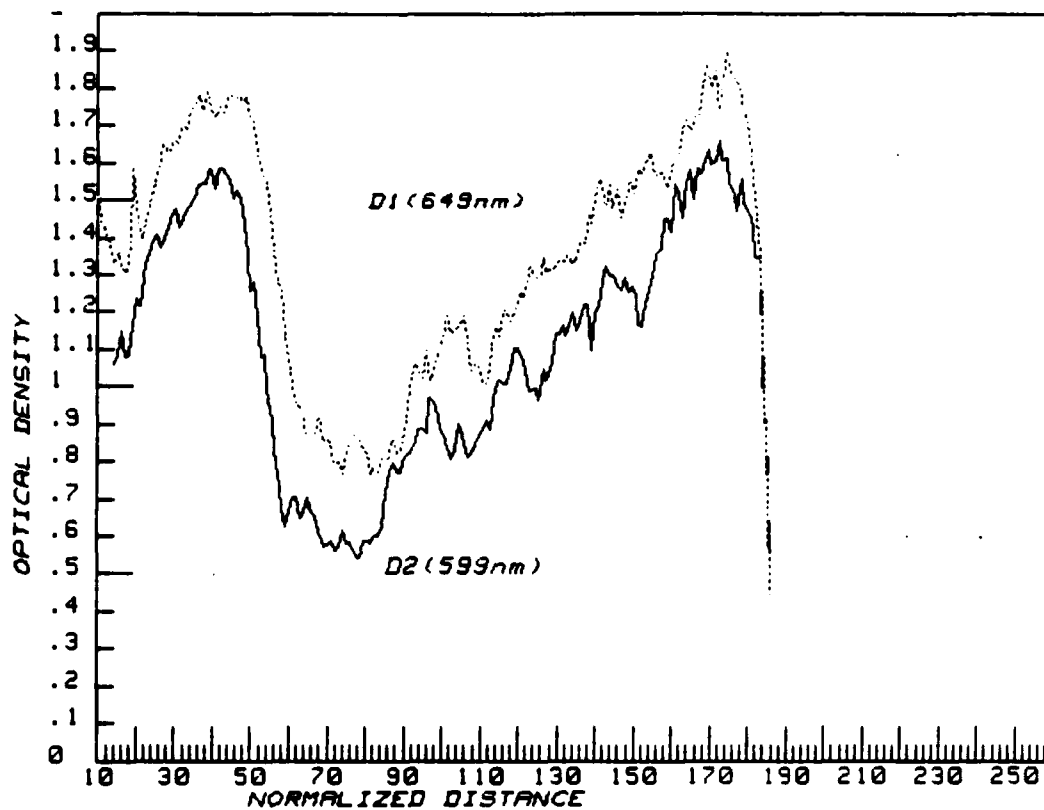Figure 9. Measured film density in wavelength of 649 nm and 599 nm as a function of normalized distance along the particle track.
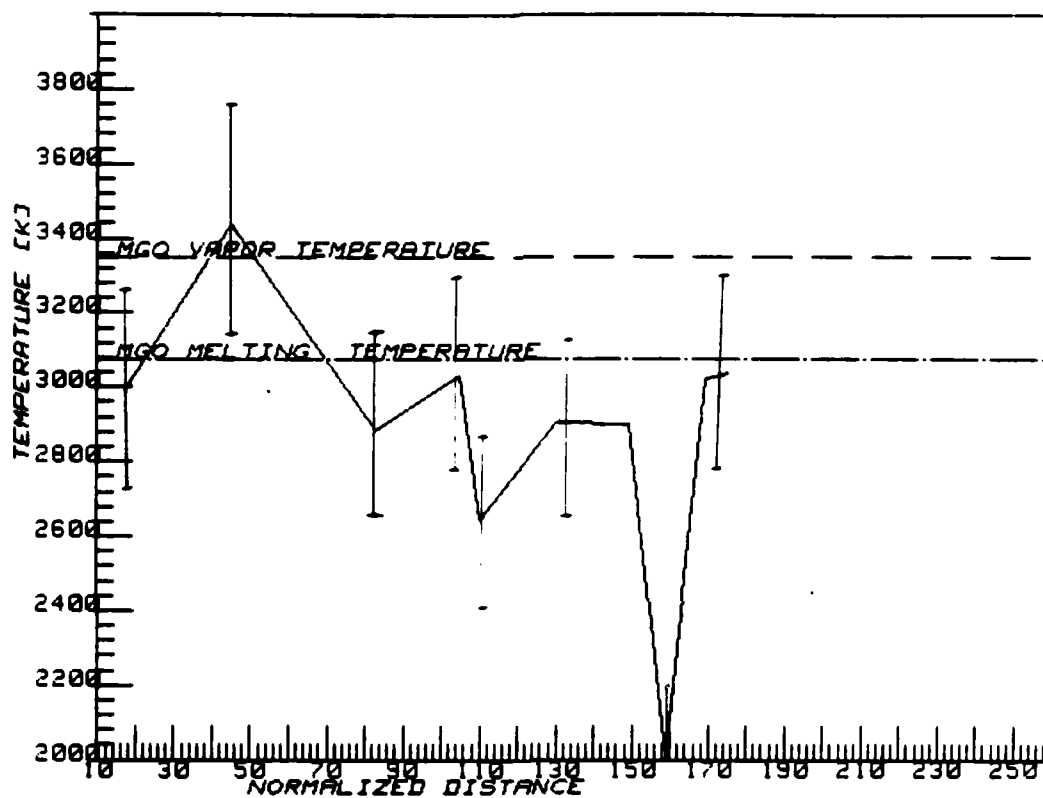
Figure 10. Typical temperature variations of magnesium particle in steam along the particle track based on the densities of Figure 9.
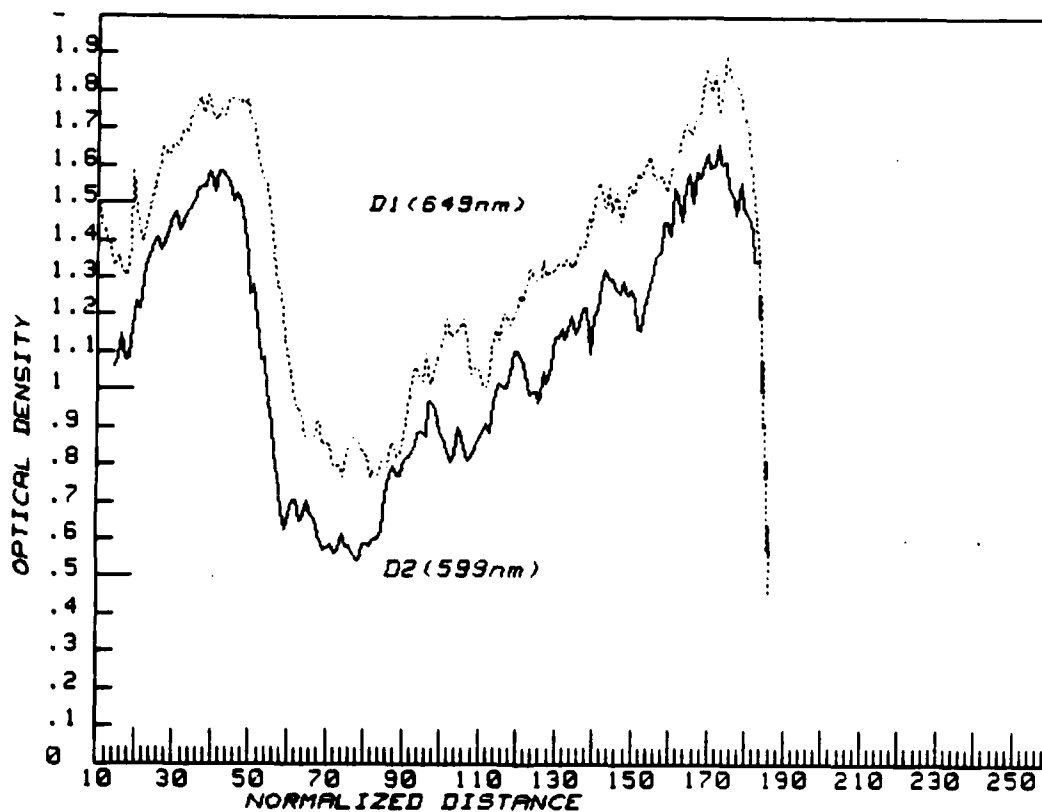
Figure 9. Measured film density in wavelength of 649 nm and 599 nm as a function of normalized distance along the particle track.

23

V. SUMMARY

The temperature measurement of magnesium particles burning in steam by using TC-PPM method can be summarized as follows: The maximum temperature of the burning particles along the track was about the boiling temperature of magnesia (3350 K). By observing the photgraphic results and the measured densities of the film, one can observe three regions of different behavior along the particle tracks as follows:

    a. The First Region

        At close range to the plasma the calculated temperature based on experimentally measured densities was about the vapor temperature of magnesia (3350 K). The radiation in this region is more intense in wavelength ranges from 482 to 450 nm compared to 649 nm. This phenomenon were found by comparing the results of measured optical densities by using different filters.

    b. The Second Region

        In this region the influence of the blue radiation which was measured at 482 nm and 450 nm, is reduced and the cooling of the particle was observed. The temperature decreased from 3430 K $\pm$ 9.1% to 3125 K $\pm$ 5.7%, while the temperature is decreased by only small amount, the changes in radiation (measured from density) in this region are relatively high; see Figure 4. The changes could be related to emissivity variations due to peeling of the magnesia as was seen also in Figures 2 and 3.

    c. The Third Region

        This region is related to the end of burning. The particle temperature is 1990 K and is below the normal freezing point of magnesia (3075 K), i.e., the magnesia is supercooled. Then suddenly

the magnesia crystallizes and returns to near the equilibrium melting temperature with abrupt increase of thermal emission that was measured as 2840 K ± 5.7%; see Figure 5.

Figure 11. Measured film density as a function of normalized distance along the particle track.
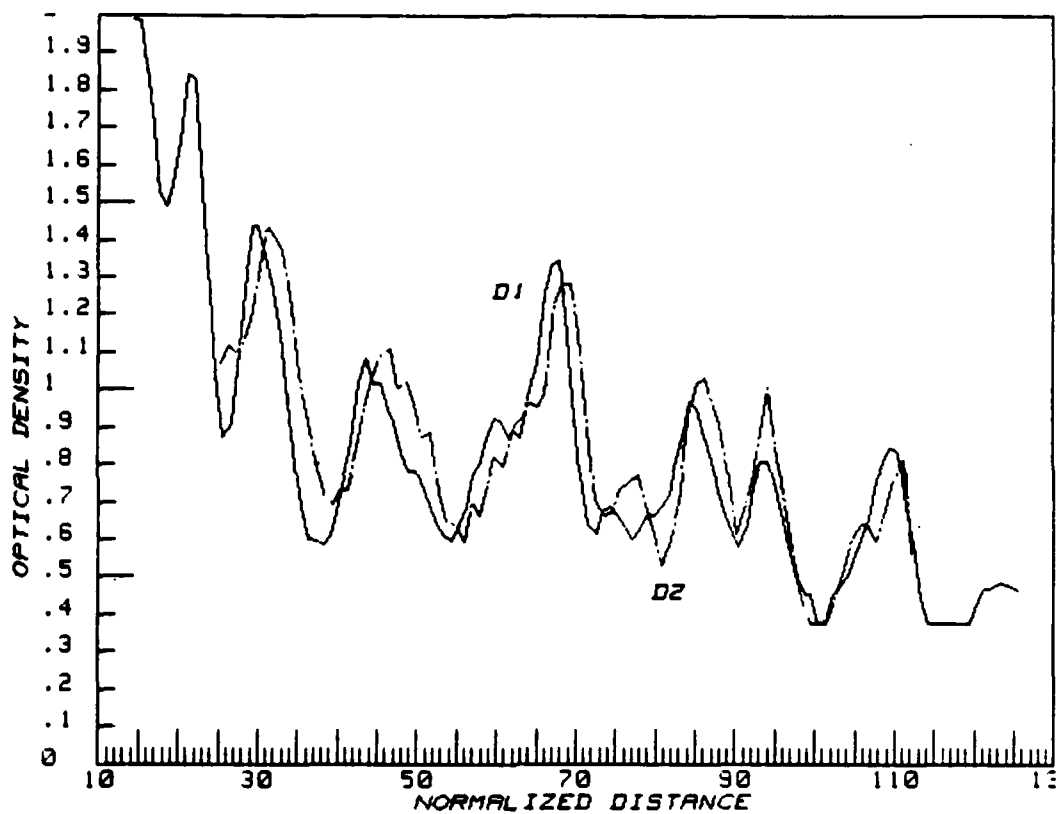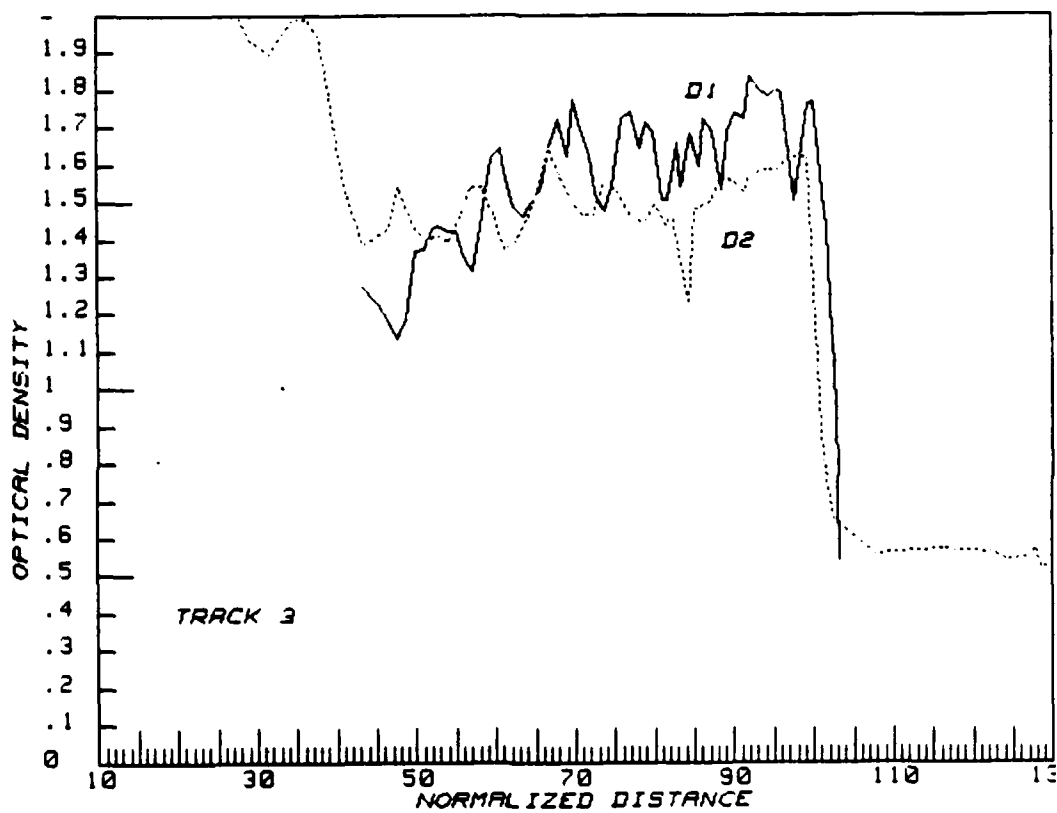
a. Track 2

Figure 11. Measured film density as a function of normalized distance along the particle track.
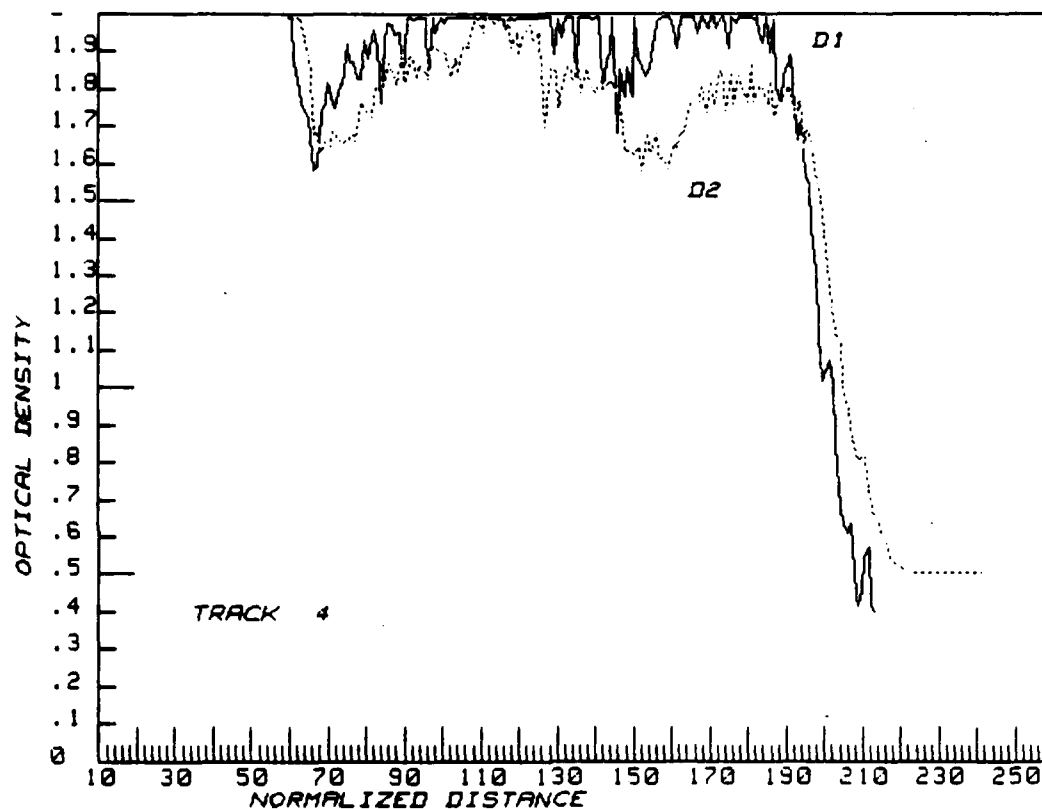
b. Track 3

Figure 11. Measured film density as a function of normalized distance along the particle track.
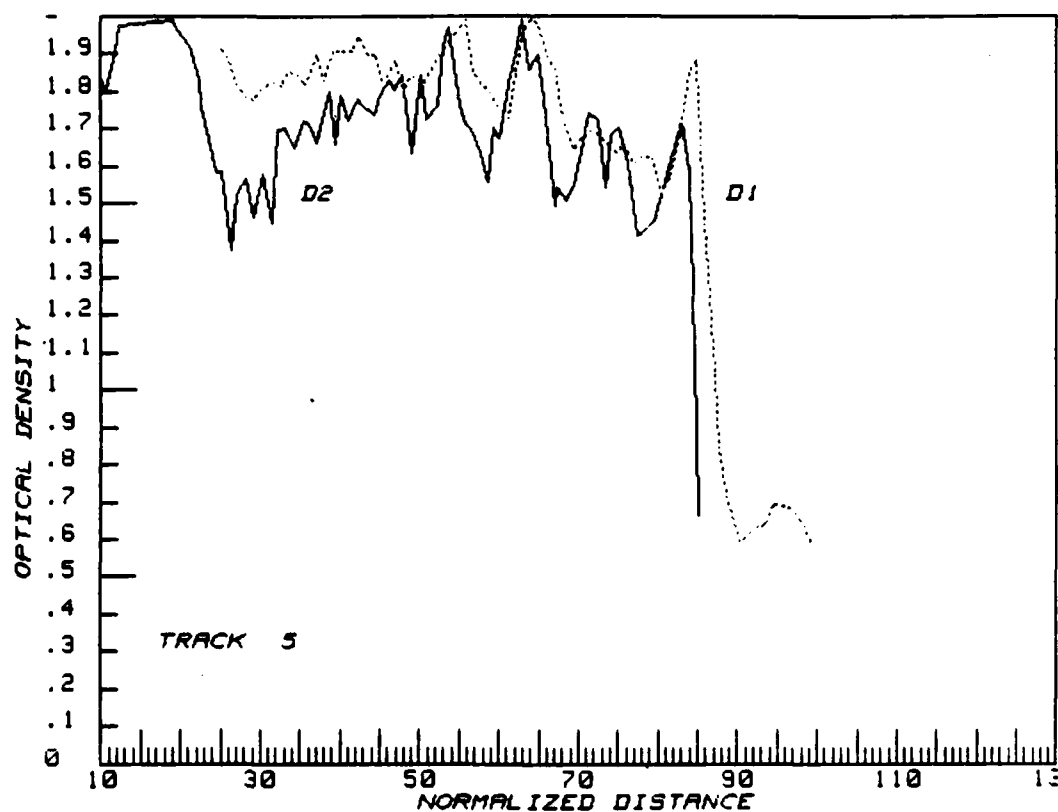
c. Track 4

Figure 11. Measured film density as a function of normalized distance along
the particle track.

d. Track 5

30

VI. REFERENCES

1. Hallenbeck, A. E., "Preliminary Investigation of Aluminum Combustion in Air and Steam", Thesis Advisor: Professor A. E. Fuhs, Naval Postgraduate School, Monterey, CA

2. Berger, M., Fuhs, A. E. and Kol, J., "Two-Color Photo-Pyrometry Method for Temperature Measurement of Moving Burning Particles", Twenty Third AIAA Aerospace Sciences Meeting, AIAA 85-0157, January 1985.

3. Kol, J., Fuhs, A. E. and Berger, M., "Experimental Investigation of Aluminum Combustion in Steam", Twenty Third AIAA Aerospace Science Meeting, AIAA 85-0323, January 1985.

4. Brzustowski, T. A. and Glassman, I., "Spectroscopic Investigation of Metal Combustion", Progress in Astronautics and Aeronautics, Volume 15, 1964, Academic Press, NY and London, pp. 41-73.

5. Brzustowski, T. A. and Glassman, I., "Vapor-Phase Diffusion Flames in Combustion of Magnesium and Aluminum. Experimental Observation in Oxygen Atmospheres," Progress in Astronautics and Aeronautics, Volume 15, 1964, Academic Press, NY and London, pp. 117-158.

6. Grosse, A. V. and Conway, J. B., "Combustion of Metals in Oxygen", Industrial and Engineering Chemistry, Volume 50, 1958, pp. 663-672.

7. Florko, A. V., Zolotko, A. N., Kaminskaya N. V. and Shevchuk V. G. "Spectral Investigation of the Combustion of Magnesium Particles", Fizika Goreniya i Vzryva, Volume 18, No. 1, January-February 1982, pp. 17-22.

8. Buber, M.; Karow, H. U. and Muller, K., "Study of Spectral Reflectivity and Emissivity of Liquid Ceramics," High Temperature-High Pressure, Vol. 12, pp. 161-168, 1980.

9. Touloukian, Y. S. and DeWitt, D. P., Thermal Radiative Properties, Plenum Publishing Company, New York, Vol. 7, 1970.

10. Kodak Publication, No. G-160, Kodak Recording Film 2475 Estar-AH Base, June 1980.

11. Robinson, J. W., Editor, CRC Handbook of Spectroscopy, published by CRC Press, 1974.

12. Herzberg, G., Spectra of Diatomic Molecules, published by D. Van Nostrand Company, Inc., 1950.

13. Pearse, R. W. B. and Gaydon, A. G., The Identification of Molecular Spectra, J. Wiley and Sons, Inc., 1963.

14. Derevyaga, M. E., Stesik, L. N. and Fedorin, E. A., "Magnesium Combustion Regimes", FGV No. 5, September-October 1978, pp. 3-10.

15. Nelson, L. S.; Rosner, D. E.; Kurzius, S. C. and Levine, H. S., "Combustion of Zirconium Droplets in Oxygen/Rare Gas Mixture-Kinetics and Mechanism", Twelfth Combustion (International) Symposium, The Combustion Institute, Pittsburgh, PA, pp. 59-69, 1969.

16. Markstein, G. H., "Magnesium-Oxygen Dilute Diffusion Flame", Ninth Symposium (International) on Combustion, Academic Press, pp. 137-148, 1963.

DISTRIBUTION LIST

No. Copies

1. Defense Technical Information Center   2
   Cameron Station
   Alexandria, Virginia 22314

2. Library, Code 0142   2
   Naval Postgraduate School
   Monterey, California 93943

3. Department Chairman, Code 67   1
   Department of Aeronautics
   Naval Postgraduate School
   Monterey, California 93943

4. Distinguished Professor Allen E. Fuhs   2
   Code 67Fu
   Naval Postgraduate School
   Monterey, California 93943

5. Mr. Donald E. Phillips, Code R10A   3
   White Oak Laboratory
   Naval Surface Weapons Center
   Silver Springs, Maryland 20910

6. Dr. Franklin D. Hains, Code R14   1
   White Oak Laboratory
   Naval Surface Weapons Center
   Silver Springs, Maryland 20910

7. Mr. Wayne K. Reed, Code R14   1
   White Oak Laboratory
   Naval Surface Weapons Center
   Silver Springs, Maryland 20910

8. Information Services Division, Code X20   1
   White Oak Laboratory
   Naval Surface Weapons Center
   Dahlgren, Virginia 22448

9. Mr. George Daniello   1
   White Oak Laboratory
   Naval Surface Weapons Center
   Silver Springs, Maryland 20910

10. Captain Robert M. Wellborn, Jr., Director   1
    Mark 50 Torpedo Office
    Naval Sea Systems Command
    Washington, DC 20360

11. Mr. Francis J. Romano, SEA 63R3   1
    Naval Sea Systems Command
    Washington, DC 20360

12. Dr. William Sykes, Code 175   1
    David W. Taylor Naval Ship Research
     and Development Center
    Bethesda, Maryland 20084

13. Mr. Raymond P. Gogolewski   1
    Defense Advanced Research Project Agency
    1400 Wilson Boulevard
    Arlington, Virginia 22209

14. Mr. Charles Beatty   1
    Naval Undersea Center
    San Diego, California 92132

15. Professor Forman Williams   1
    Princeton University
    Princeton, New Jersey 08540

16. LCDR Amos E. Hallenbeck, Jr.   2
    3293 Edinburgh Drive
    Virginia Beach, Virginia 23452

17. Jonathan L. Minner   1
    Naval Surface Weapons Center
    Dahlgren, Virginia 22448

18. Zernow Technical Services   1
    Attn: Louis Zernow
    425 West Bonita
    San Dimas, California 91773

19. Dr. Louis Baker, Jr.   1
    Argonne National Laboratories
    9700 South Cass Avenue
    Building 207
    Argonne, Illinois 60439

20. Professor Irvin Glassman   1
    Department of Mechanical and
     Aeronautical Engineering
    Princeton University
    Princeton, New Jersey 08540

21. R. G. S. Sewell   1
    Code 3835
    Naval Weapons Center
    China Lake, California 93555

22. R. R. Durrell   1
    Code R12
    Naval Surface Weapons Center
    Silver Springs, Maryland 20910

23. LT Jerome Buck   1
    USS Goldsborough (DDG-20)
    FPO, San Francisco 96666

24. LT John Strott   1
    USS Radford (DD-968)
    FPO, New York 09586

25. D. R. Kennedy Associates, Inc.   1
    4940 El Camino Real, Suite 209
    Post Office Box 4003
    Mountain View, California 94040

26. Mr. J. M. McNerney   1
    Battelle
    Columbus Laboratories
    505 King Avenue
    Columbus, Ohio 43201

27. Dr. G. E. Jensen   1
    Chemical Systems Division
    United Technology Corporation
    Post Office Box 358
    Sunnyvale, California 94086

28. Dr. Edward G. Liszka   1
    Mark 50 Torpedo Office
    Naval Sea Systems Command
    Washington, DC 20360

29. Mr. Mati Berger   1
    Ministry of Defense
    P.O. Box 2250
    Haifa, Israel

30. Mr. Jacob Kol (88)   1
    Ministry of Defense
    P.O. Box 2250
    Haifa, Israel

31. Professor C. K. Law   1
    Department of Mechanical Engineering
    University of California at Davis
    Davis, CA 95616

32. Mr. Yair Chozev (87)   1
    Ministry of Defense
    P.O. Box 2250
    Haifa, Israel

35

33. Professor A. Gany   1
    Department of Aeronautical Engineering
    Technion
    Haifa, Israel

34. Dr. Norman Hubele   1
    Mail Stop 1301-R
    GPSD
    2801 E. Washington
    Phoenix, AZ 85034

35. Professor Paul Dimotakis   1
    California Institute of Technology
    301-46
    Pasadena, CA 91125

36. Research Administration Office   1
    Code 012A
    Naval Postgraduate School
    Monterey, CA 93943

END

FILMED

10-85

DTIC